

Fluorine nucleosynthesis and s-processing in AGB stars driven by magnetic-buoyancy mixing

Diego Vescovi^{1,*}, Sergio Cristallo^{2,3}, Sara Palmerini^{3,4}, Carlos Abia⁵, and Maurizio Busso^{3,4}

¹Goethe University Frankfurt, Max-von-Laue-Strasse 1, Frankfurt am Main 60438, Germany

²INAF, Observatory of Abruzzo, Via Mentore Maggini snc, 64100 Teramo, Italy

³INFN, Section of Perugia, Via A. Pascoli snc, 06123 Perugia, Italy

⁴Department of Physics and Geology, University of Perugia, via A. Pascoli snc, 06123 Perugia, Italy

⁵University of Granada, Departamento de Física Teórica y del Cosmos, 18071 Granada, Spain

Abstract. Asymptotic giant branch (AGB) stars are thought to be among the most important sources of fluorine in our Galaxy. While observations and theory agree at close-to-solar metallicity, stellar models overestimate fluorine production in comparison to heavy elements at lower metallicities. We present predictions for ^{19}F abundance for a set of AGB models with various masses and metallicities, in which magnetic buoyancy induces the formation of the ^{13}C neutron source (the so-called ^{13}C pocket). In our new models, fluorine is mostly created as a consequence of secondary ^{14}N nucleosynthesis during convective thermal pulses, with a minor contribution from the ^{14}N existing in the ^{13}C pocket zone. As a result, AGB stellar models with magnetic-buoyancy-induced mixing show low ^{19}F surface abundances which agree with fluorine spectroscopic observations at both low and near-solar metallicity.

1 Introduction

The cosmic genesis of fluorine is one of the most intriguing problems in nuclear astrophysics. So far, spectroscopic observations of photospheric F enhancements in intrinsic AGB carbon stars [1, 2] and metal-poor extrinsic stars [3, 4] offer the sole direct observation of fluorine production. Its envelope abundance indicates a correlation with those of carbon and s-process elements and therefore with the ^{13}C content produced in the interiors of AGB stars [5]. Recently, it was proposed that a process resulting in the creation of an extended ^{13}C pocket and, simultaneously, a tiny quantity of ^{14}N , may solve the issue of ^{19}F overproduction with respect to s-elements in low-mass metal-poor objects [4].

The formation of a ^{13}C pocket in AGB stars requires that some partial mixing of protons from the envelope occurs during a third dredge-up (TDU) phenomenon. In latest FRUITY models [6], the buoyant rise of magnetic flux tubes in the region below the envelope is considered to cause a stable mass upflow which induces a downflow of protons for maintaining mass conservation. As a result of such magnetic mixing, deep profiles of low proton abundances are predicted to be formed. Because protons are nearly completely used for the synthesis of ^{13}C , the low proton concentration significantly reduces the local ^{14}N formation, thereby limiting ^{19}F production as well. Here we examine fluorine nucleosynthesis in low-mass AGB

*e-mail: vescovi@iap.uni-frankfurt.de

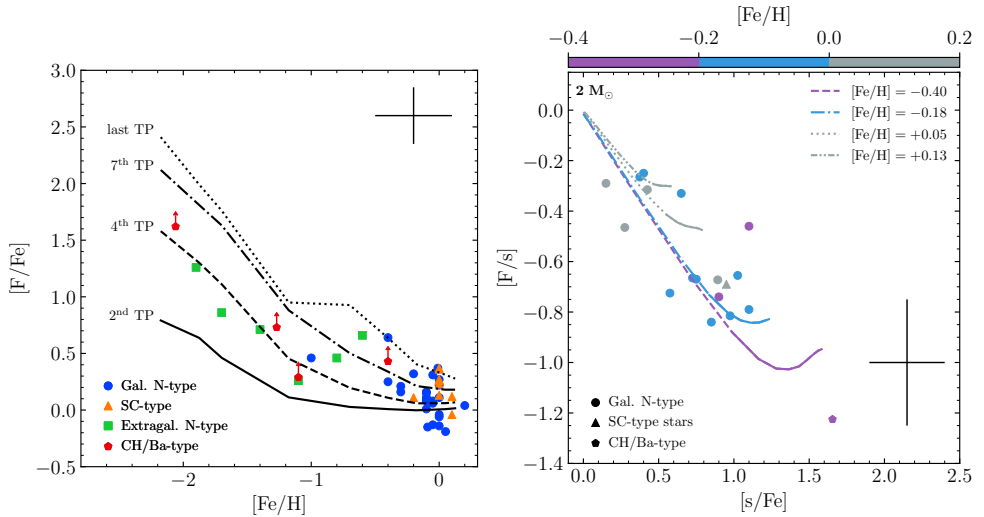


Figure 1. (Left panel) Comparison between observed $[F/Fe]$ ratios as a function of the metallicity and FRUITY magnetic models. Symbols refer to four data groups: circles, galactic (N-type) carbon stars; triangles, SC-type stars; squares, extragalactic carbon stars; pentagons, extrinsic CH/Ba stars. Lines represent theoretical predictions for 2 (for $[Fe/H] \geq -0.7$) and $1.5 M_{\odot}$ (for $[Fe/H] < -0.7$) AGB stars at different thermal pulses (TPs). (Right panel) Observed $[F/s]$ vs. average s-element enhancements compared with theoretical predictions for $2 M_{\odot}$ and close-to-solar metallicity models. Data points and theoretical lines are color-coded by $[Fe/H]$. The solid portion of the lines represents the theoretical C-rich phase, while the dashed portion represents the O-rich phase. Typical error bars are indicated.

stars by computing a new series of stellar models accounting for the formation of a magnetic-buoyancy-induced ^{13}C pocket.

2 Comparison with observations

In the following, we compare data for intrinsic AGB carbon stars [2, 4] and extrinsic CH/Ba stars [4, 5] with new FRUITY magnetic models of $1.5 M_{\odot}$ and $2 M_{\odot}$.

In left panel of Fig. 1 we report the $[F/Fe]$ ratios of the selected sample as a function of $[Fe/H]$. Within the observational errors, there is a good agreement, confirming the expected F-enhancement trend with the metallicity. The right panel of Fig. 1 shows the comparison between theoretical predictions of FRUITY magnetic models and spectroscopic observations for $[F/s]$ ratios vs. the average s-element enhancement. In this way, the F enhancement for the extrinsic stars is not affected by uncertainties related to the dilution factor and provides a robust tool for comparison. Theoretical expectations can replicate the quasi-linear decreasing trend of $[F/s]$ with the surface s-process enrichment.

In Fig. 2 we perform a similar comparison at low metallicities. We compared model predictions individually since there is no homogeneous sample of stars with both Ba and La. Magnetic models well reproduce the spread observed at different metallicities for both $[F/Ba]$ and $[F/La]$ ratios as a function of total s-process enhancement. Overall, FRUITY magnetic models show a reduction in fluorine production that is consistent with spectroscopic observations of low-metallicity stars. The extended profile and low proton abundance that characterize FRUITY magnetic models [6] have the dual impact of generating large ^{13}C pockets and a small amount of primary ^{14}N . In this scenario, the few available protons make

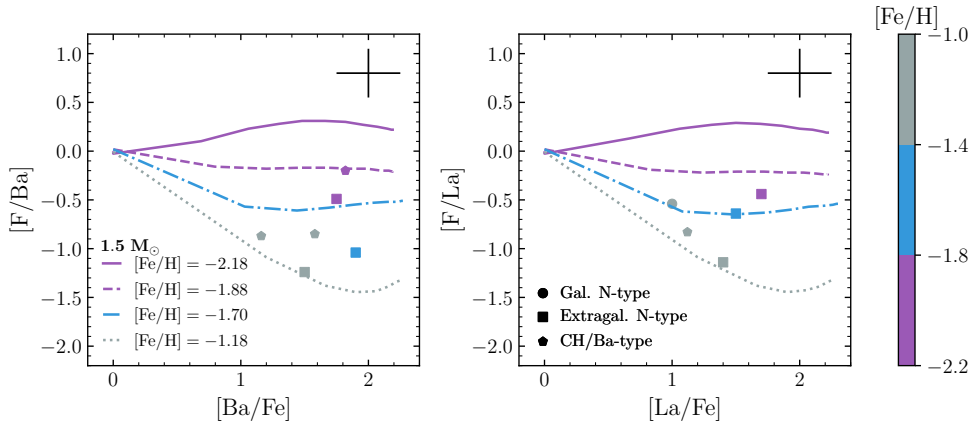


Figure 2. [F/Ba] vs. [Ba/Fe] (left panel) and [F/La] vs. [La/Fe] (right panel) in the sample stars with $[\text{Fe}/\text{H}] \leq -1.0$. Symbols as in Fig. 1. Note that at these low metallicities, theoretical AGB models predict that the star becomes C-rich from first TDU episodes. Data points and theoretical lines are color-coded by [Fe/H]. Typical error bars are indicated.

first ^{13}C through the $^{12}\text{C}(p, \gamma)^{13}\text{C}$ reaction, preventing further proton captures to form ^{14}N , thus inhibiting the nuclear chain $^{14}\text{N}(n, p)^{14}\text{C}(\alpha, \gamma)^{18}\text{O}(p, \alpha)^{15}\text{N}(\alpha, \gamma)^{19}\text{F}$. As a consequence, any fluorine appearing in AGB envelopes in these models is of secondary origin, caused by ^{14}N concentrations left over after H-shell burning. As an outcome, FRUITY magnetic models have low fluorine enhancements and large s-enhancements, which are in close agreement with observations in very metal-poor AGB stars [7].

3 Conclusions

The production of fluorine in low-mass AGB stars has been examined in light of new FRUITY stellar models, in which the ^{13}C neutron source is attributed to magnetic-buoyancy-induced phenomena. On the one hand, the new FRUITY magnetic models exhibit a low net ^{19}F production. This is due to the low abundance of ^{14}N in the ^{13}C pocket, which results in negligible fluorine production during ^{13}C radiative burning. The ^{19}F envelope abundance is therefore ascribed only to the amount of the secondary ^{13}C in the H-shell ashes, which depends on the CNO abundances in the star. On the other hand, mixing induced by magnetic buoyancy leads to extended ^{13}C pockets so resulting in large surface s-process enrichments. As a whole, new FRUITY magnetic models simultaneously account for both the observed fluorine and the average s-element enhancements in intrinsic AGB carbon stars and extrinsic CH/Ba stars.

References

- [1] A. Jorissen, V.V. Smith, D.L. Lambert, *A&A* **261**, 164 (1992)
- [2] C. Abia, K. Cunha, S. Cristallo, P. de Laverny, *A&A* **581**, A88 (2015)
- [3] S. Lucatello, T. Masseron, J.A. Johnson, M. Pignatari, F. Herwig, *ApJ* **729**, 40 (2011)
- [4] C. Abia, S. Cristallo, K. Cunha, P. de Laverny, V.V. Smith, *A&A* **625**, A40 (2019)
- [5] M. Forestini, S. Goriely, A. Jorissen, M. Arnould, *A&A* **261**, 157 (1992)
- [6] D. Vescovi, S. Cristallo, M. Busso, N. Liu, *ApJL* **897**, L25 (2020)
- [7] D. Vescovi, S. Cristallo, S. Palmerini, C. Abia, M. Busso, *A&A* **652**, A100 (2021)